IOPscience iopscience.iop.org

Home Search Collections Journals About Contact us My IOPscience

First- and second-order Raman scattering of the $Al_xGa_{1-x}Sb$ alloy for x=0.14

This article has been downloaded from IOPscience. Please scroll down to see the full text article.

1995 J. Phys.: Condens. Matter 7 7069

(http://iopscience.iop.org/0953-8984/7/35/014)

View the table of contents for this issue, or go to the journal homepage for more

Download details:
IP Address: 171.66.16.151
The article was downloaded on 12/05/2010 at 22:03

Please note that terms and conditions apply.

J. Phys.: Condens. Matter 7 (1995) 7069–7076. Printed in the UK

First- and second-order Raman scattering of the $Al_xGa_{1-x}Sb$ alloy for $x = 0.14$

R Cuscó†, L Artús† and K W Benz‡

† Institut Jaume Almera, Consell Superior d'Investigacions Científiques (CSIC), Lluís Solé i Sabarís sin numero, 08028 Barcelona, Spain

‡ Kristallographisches Institut, Albert-Ludwigs-Universität Freiburg, Hebelstrasse 25, D-79104 Freiburg, Germany

Received 11 April 1995, in final form 7 June 1995

Abstract. First- and second-order Raman spectra of the $Al_xGa_{1-x}Sb$ alloy for $x = 0.14$ have been measured. High-resolution Raman spectra performed at 80 K allowed us to resolve the TO–LO splitting of both GaSb-like and AlSb-like modes. The values of TO–LO splitting we measured suggest the occurrence of charge transfer from the Ga–Sb bond to the Al–Sb bond, which in this alloy is mainly governed by the different cation electronegativities. The AlSb-like LO peak is substantially broader than its GaSb-like counterpart, reflecting a much higher degree of disorder in the AlSb sublattice as a consequence of the low Al concentration of the sample studied in this work. In the second-order Raman spectrum, three frequency regions can be clearly distinguished, containing, respectively, overtones and combinations of GaSb-like modes, combinations of GaSb-like and AlSb-like modes, and overtones of AlSb-like modes.

1. Introduction

Recently, the $Al_xGa_{1-x}Sb$ alloy has attracted much interest as a constituent of the InAs–(Ga, Al)Sb system for its possible applications in bandstructure engineering. It is known that in the type II InAs–GaSb heterostructure the top of the GaSb valence band lies higher in energy than the bottom of the InAs conduction band, giving rise to the coexistence of electrons and holes separated at the interfaces [1]. The bandgap of the $Al_xGa_{1-x}Sb$ alloy increases with the Al composition, allowing the band offset of InAs–(Ga, Al)Sb heterostructures to be engineered by changing the substitutional species composition. In fact, a strong decrease of hole concentration with increasing Al composition, reaching zero at about $x = 0.3$, has been reported [2], which demonstrates the crossing of the valence band edge of $Al_xGa_{1-x}Sb$ and the conduction band edge of InAs at that alloy composition.

The small lattice mismatch of the alloy with respect to the InAs lattice and the low effective mass of the electrons in InAs favour high electron mobility in InAs–(Ga, Al)Sb-based devices. Electron mobility values in excess of 10^5 cm^2 V^{-1} s^{-1} below 4.2 K have been reported in InAs–(Ga, Al)Sb quantum well structures for a wide compositional range [2]. Moreover, the type II bandstructure of the InAs–(Ga, Al)Sb system with its large band offset and the possibility of setting the InAs conduction band edge slightly below the midgap of (Ga, Al)Sb, where the tunnelling probability is minimum, together with the low-resistance InAs electrodes, make the system ideal for negative differential resistance tunnelling devices, with applications in microwave and millimetre wave detectors and amplifiers. Negative differential resistance was observed in $Al_xGa_{1-x}Sb$ single-barrier

0953-8984/95/357069+08$19.50 © 1995 IOP Publishing Ltd

tunnelling devices at 100 K [3]. Short tunnelling times and wide negative differential resistance (NDR) regions can be achieved in these structures, favouring the observation of negative differential resistance at room temperature, as demonstrated by the measurements of Beresford *et al* [4] and Söderström *et al* [5]. Also, the characteristic alignment of the bands in InAs–(Ga, Al)Sb-based structures has been used to produce a novel intrinsic-current bistability in a double-barrier tunnelling device [6]. The high mobility and strong confinement of the electrons in an InAs–(Ga, Al)Sb well can be advantageously used in the pursuit of mesoscopic devices operating at higher temperatures. The observation of quantized conductance in InAs–(Ga, Al)Sb quantum wires at 80 K has been recently reported [7].

$Al_xGa_{1-x}Sb$ is also used in the field of optical communications as a constituent of (Ga, Al)Sb–GaSb-based lasers operating in the region of minimal absorption and dispersion in optical fibres. Tsang and Olsson [8] reported 1.78 μm wavelength $Al_{0.2}Ga_{0.8}Sb$/GaSb double-heterostructure lasers, and Ohmori *et al* [9] reported room-temperature lasing operation of an $Al_{0.2}Ga_{0.8}Sb$/GaSb multi-quantum-well laser at 1.646 μm.

Despite the increasing interest in (Ga, Al)Sb-related systems there is a poor knowledge of the phonons of the alloy. The most complete study of phonons in $Al_xGa_{1-x}Sb$ available so far is the set of room-temperature infrared reflectivity measurements by Lukovsky *et al* [10], in which a two-mode behaviour was found over the entire compositional range of the alloy. Only one paper on Raman scattering measurements on $Al_xGa_{1-x}Sb$ can be found [11], which displays only partial second-order Raman spectra for different composition alloys without identification of the observed structures. On the theoretical side, the two-mode behaviour was obtained from a concentration-dependent mixing parameter model [12], and a Green function treatment incorporating an eleven-parameter rigid-ion model aimed at studying impurity-induced structure was developed by Talwar *et al* [13].

In this paper we present the first Raman scattering study of the long-wavelength phonons of the $Al_xGa_{1-x}Sb$ alloy for $x = 0.14$. A two-mode behaviour was found for this alloy composition, and TO–LO splitting of both GaSb-like and AlSb-like modes could be resolved in the high-resolution first-order Raman spectra. Although the TO–LO splitting of AlSb-like modes was already visible at room temperature, further measurements were carried out at 80 K in order to improve the resolution and clearly separate the transverse and longitudinal optical AlSb-like phonons of such a low-Al-composition alloy. We also report second-order Raman spectra that show structures associated with GaSb-like modes, AlSb-like modes, and combinations of both.

2. Experiment

The measurements were performed on a (111) face of a high-quality bulk $Al_{0.14}Ga_{0.86}Sb$ crystal. The undoped crystals, with a diameter of 24 mm, were grown by the travelling heater method (THM) in quartz ampoules using Sb-rich solution zones. The growth temperature was about 580 °C, and the pulling rate of the ampoule was about 1 mm d^{-1}. A more detailed description of the growth process has been published elsewhere [14].

The 488 nm line of an Ar^+ laser was used as excitation, with an incident power of 100 mW, and the scattered light was analysed by a T64000 Jobin–Yvon spectrometer equipped with a charge-coupled device (CCD) detector cooled with liquid nitrogen. Full-range spectra were recorded in the subtractive configuration, with 100 μm slits. High-resolution measurements aimed at resolving first-order TO–LO splittings were performed using the triple-additive configuration with 60 μm slits, providing a resolution better than 1 cm^{-1}. The unpolarized spectra were recorded in backscattering geometry, in which,

according to selection rules, both TO and LO modes are allowed. A liquid nitrogen cryostat from TBT Air Liquide was used for the measurements at 80 K. In the low-frequency-range measurements, the sample area was purged using a continuous Ar flow in order to suppress the Raman lines arising from atmospheric interactions.

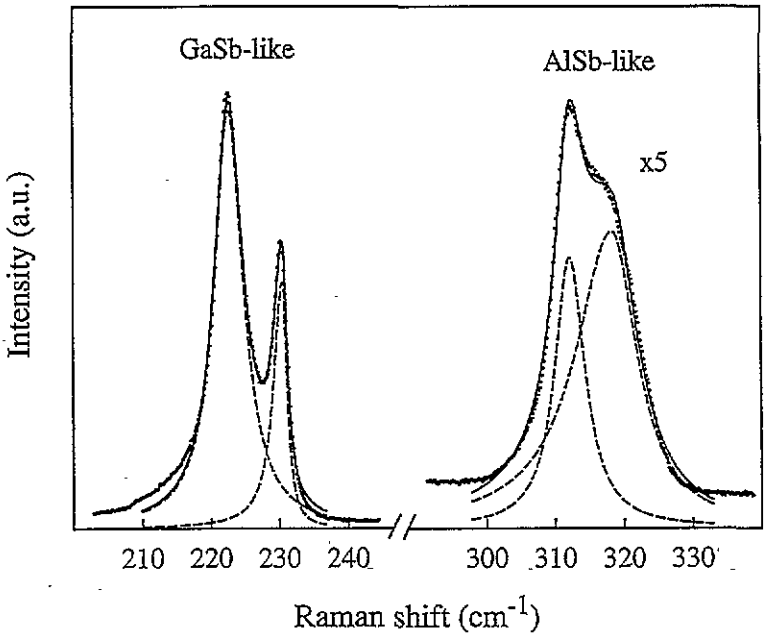

Figure 1. First-order Raman spectrum of $Al_{0.14}Ga_{0.86}Sb$ at room temperature, with resolution better than 1 cm^{-1}. Lorentzian line shapes (solid line) have been fitted to the experimental data (dots). The dashed lines represent the separate TO and LO contributions to the fitted curves.

3. Discussion

In figure 1 we show the room-temperature first-order Raman scattering of GaSb-like and AlSb-like modes. The frequencies of the GaSb-like modes can be determined directly from the measured spectrum, and we find $\omega_{TO} = 223$ cm^{-1} and $\omega_{LO} = 230$ cm^{-1}. For the overlapping AlSb-like modes, we observe a distinct peak at 312 cm^{-1} corresponding to the TO mode, and a shoulder on its high-energy side which corresponds to the LO mode. In order to obtain a more accurate value of the LO mode frequency, Lorentzian line shape fits to the experimental points were carried out, resulting in a LO mode frequency value of 318 cm^{-1}. From the least-squares fits we also obtained an estimation of the widths of the overlapping TO and LO peaks, which were found to be ≈ 5 and ≈ 11 cm^{-1}, respectively. The frequencies we report are in excellent agreement with the values obtained by Lukovsky *et al* [10] from a damped harmonic oscillator fit to their infrared reflectivity data on $Al_{0.15}Ga_{0.85}Sb$. Since in backscattering geometry, according to polarization selection rules, the TO mode is always allowed in Raman scattering from a (111) face, the LO AlSb-like mode cannot be detected separately from its TO counterpart as a single peak by means of polarization analysis. In view of the fact that the AlSb-like LO peak is not well resolved because of the large widths of the AlSb-like modes, we performed measurements at 80 K with resolution better than 1 cm^{-1} aimed at reducing the phonon linewidth and allowing a

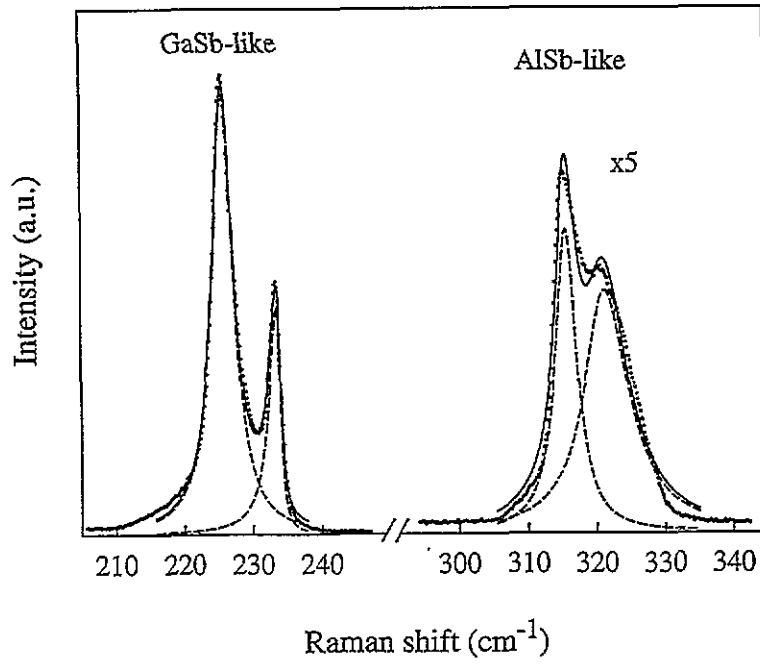

Figure 2. As figure 1, but for the spectrum at 80 K.

direct experimental measurement of the frequency of the AlSb-like LO peak. In figure 2 we show the first-order Raman spectrum of $Al_{0.14}Ga_{0.86}Sb$ at 80 K with resolution better than 1 cm^{-1}. As can be seen in this figure, TO and LO AlSb-like modes were experimentally resolved, and unambiguously found at $\omega_{TO} = 315$ cm^{-1} and $\omega_{LO} = 321$ cm^{-1}. GaSb-like modes were found at $\omega_{TO} = 226$ cm^{-1} and $\omega_{LO} = 233$ cm^{-1}. Both AlSb-like and GaSb-like first-order optical modes are shifted to higher energies by $\approx$3 cm^{-1} in agreement with the temperature dependence $d\omega/dT = (-1.35 \pm 0.1) \times 10^{-2}$ cm^{-1} K^{-1} found by Jusserand and Sapriel [15] for the identical-cation alloy $Al_xGa_{1-x}As$. Consequently, the TO–LO splitting values measured at low temperature are unchanged from their corresponding values at room temperature, and the improved definition of the AlSb-like LO peak at 80 K is due to the narrowing of the phonon peaks at lower temperatures. In fact, Lorentzian line shape fits to the low-temperature, AlSb-like TO and LO peaks yield values of full width at half height of 4 and 8 cm^{-1} respectively, in contrast with the values 5 and 11 cm^{-1} found at room temperature. In table 1 we summarize our results on first-order Raman scattering of $Al_{0.14}Ga_{0.86}Sb$. The two-mode behaviour of $Al_xGa_{1-x}Sb$ is consistent with the fact that the two necessary requirements for such behaviour are satisfied. First, the frequency of the LO mode in pure GaSb at 233 cm^{-1} [16] allows the existence of a GaSb:Al local mode, which was experimentally observed at 317 cm^{-1} by infrared absorption measurements [17] and theoretically calculated at 318 cm^{-1} [18]. Second, the gap which exists between acoustic and optical branches of AlSb between 132 and 297 cm^{-1} [19] allows the existence of an AlSb:Ga gap mode, reported by Talwar and Agrawal [20] to occur at $\approx$212 cm^{-1}.

As can be seen in figures 1 and 2, whereas GaSb-like modes exhibit a clear TO–LO splitting, their AlSb-like counterparts are not easily separated, even though the magnitudes of their respective splittings are quite similar (see table 1). As already mentioned, the difficulty in resolving TO and LO AlSb-like modes arises from the large width of the LO AlSb-like mode which actually overlaps the TO AlSb-like mode. The substantial difference

Table 1. Frequencies and full widths at half height of the first-order Raman peaks of $Al_{0.14}Ga_{0.86}Sb$. The values of full width at half height (Γ) and the AlSb-like LO mode frequency at room temperature (RT) were obtained from least-squares fits of Lorentzian line shapes to the experimental data. All the other values were determined directly from the experimental spectra.

	ω_{TO} (cm^{-1})	Γ_{TO} (cm^{-1})	ω_{LO} (cm^{-1})	Γ_{LO} (cm^{-1})	TO–LO splitting (cm^{-1})
GaSb-like (RT)	223	5	230	2	7
GaSb-like (80 K)	226	4	233	2	7
AlSb-like (RT)	312	5	318	11	6
AlSb-like (80 K)	315	4	321	8	6

between the widths of the two LO modes reflects the different extent to which each sublattice is ordered, as one would expect from the relative content of each cation in the alloy. It must be underlined that the LO GaSb-like peak displays a width of only 2 cm^{-1}, which is quite small for an alloy system. This narrow LO GaSb-like peak suggests that a long-range order exists in the crystal, as found in other III–V alloy systems by electron diffraction experiments [21, 22, 23].

In spite of the more ionic character of the Al–Sb bond in relation to the Ga–Sb bond, reflected in the larger TO–LO splitting of pure AlSb, the substantial difference in the relative concentration of each cation in the $Al_{0.14}Ga_{0.86}Sb$ alloy led us to expect the difference between the magnitudes of TO–LO splitting of GaSb-like and AlSb-like modes to be larger than the value experimentally found. In particular, the TO–LO splitting around 6 cm^{-1} measured for the AlSb-like modes is far higher than the expected value of $\approx$3 cm^{-1} obtained from a linear variation with composition, using the end-point-compound value reported by Lukovsky *et al* [10]. Also, the value of $\approx$7 cm^{-1} found for the splitting of GaSb-like modes is slightly lower than the value of $\approx$8 cm^{-1} expected from a linear variation. These results suggest the existence of charge transfer from the Ga–Sb bond to the Al–Sb bond, as found for other pairs of inequivalent bonds in III–V alloys [24]. In general, this charge transfer process is attributed to two mechanisms, namely the different cation electronegativities and the structural relaxation to accommodate two different bondlengths [24]. Since no extended x-ray absorption fine-structure (EXAFS) measurements exist on $Al_xGa_{1-x}Sb$, experimental bondlength values are not available for this alloy. However, EXAFS measurements performed on $Ga_{1-x}In_xAs$ have shown that bondlengths present a bimodal distribution centred around the values of the binary components and that the maximum variation of bondlengths throughout the composition range is about 25% of the difference between those values [25]. In the case of the $Ga_{1-x}Al_xSb$ alloy, the bondlength difference between the end-point compounds is only of $\approx$0.7% [26]. Thus, assuming a compositional bondlength variation similar to that of $Ga_{1-x}In_xAs$, and taking into account the Al composition of the sample studied, we can estimate the difference between inequivalent bondlengths to be only around 0.5%. Such a small structural distortion is expected to induce a negligible charge redistribution so that, in the present case, the different cation electronegativities play the dominant role in determining the charge transfer from the less ionic Ga–Sb bond to the more ionic Al–Sb bond. Therefore, the observed values of TO–LO splitting, higher than expected for the AlSb-like modes and lower than expected for the GaSb-like modes, may be explained by the redistribution of electric charge between Ga–Sb and Al–Sb bonds.

Figure 3 shows the full Raman spectrum of $Al_{0.14}Ga_{0.86}Sb$ in the frequency region

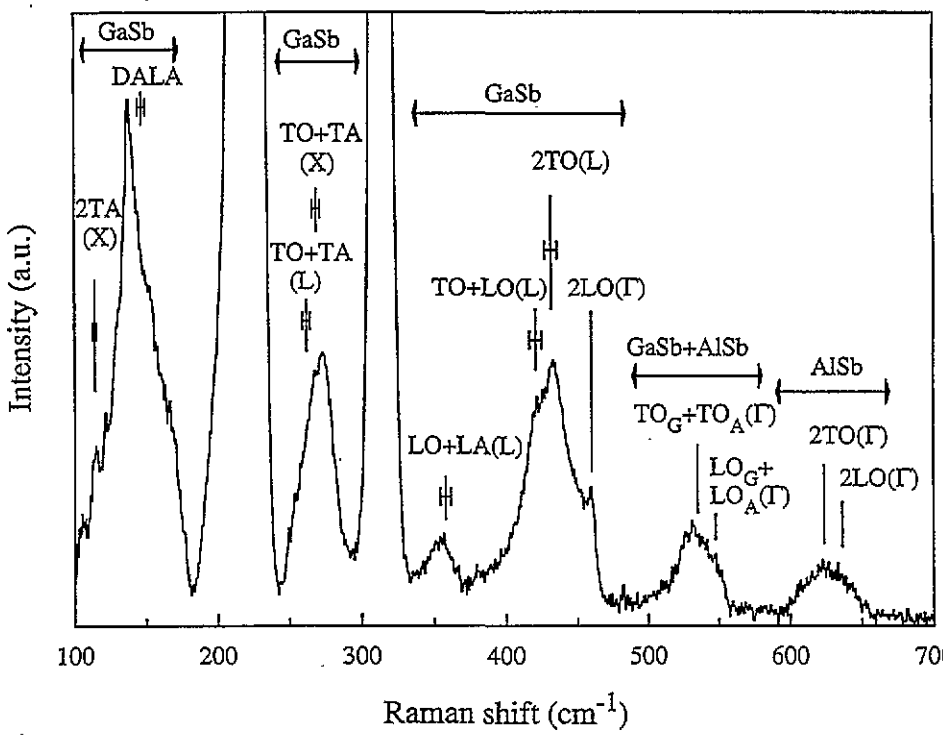

Figure 3. Second-order Raman spectrum of $Al_{0.14}Ga_{0.86}Sb$ at room temperature. In the figure the possible two-phonon contributions to the second-order spectrum are displayed, and the corresponding sums of frequencies of the modes involved are indicated by vertical lines. The frequencies of zone-centre modes were taken from the first-order Raman scattering results reported in this work. For the frequencies of zone edge modes, we have considered the neutron inelastic scattering data on pure GaSb reported by Farr *et al* [27], and the corresponding error bars are also displayed. The subscripts G and A stand for GaSb-like and AlSb-like modes respectively.

between 100 and 700 cm^{-1} where, beside the dominant first-order modes discussed above, second-order Raman modes can be observed. The assignment of the structures displayed in figure 3 was made on the basis of the first-order Raman scattering results reported in this work and of previously reported results on lattice dynamics of GaSb and AlSb. Phonon dispersion curves of GaSb were experimentally determined by neutron inelastic scattering by Farr *et al* [27]. No neutron inelastic scattering experiments have been reported on AlSb, and we have considered the phonon dispersion curves of AlSb calculated by Banerjee and Varshni [28] and the multiphonon infrared absorption data from Turner and Reese [19].

In the frequency range of 100–500 cm^{-1}, the second-order Raman spectrum of the alloy resembles that of pure GaSb [29], as could be expected from the high Ga content of the alloy. The four bands observed in the regions 100–170 cm^{-1}, 240–290 cm^{-1}, 330–370 cm^{-1}, and 380–470 cm^{-1} correspond, respectively, to overtones of transverse acoustic modes, combinations of transverse acoustic and optical modes, combinations of longitudinal acoustic and optical modes, and combinations and overtones of optical modes. The 2LO(Γ) frequency at 460 cm^{-1} sets the upper limit of the second-order spectrum of GaSb. The maximum of the band in the 120–170 cm^{-1} region is found at a higher frequency than the 2TA(X) and 2TA(L) frequencies of GaSb derived from the neutron inelastic scattering

data of Farr *et al* [27]. Given that the calculated frequency for the 2TA(L) mode in AlSb is 134 cm^{-1} [28], a possible contribution of AlSb overtones of transverse acoustic modes cannot be ruled out. This band also displays two shoulders on its high-frequency side, which coincide with maxima of the density of states of longitudinal acoustic modes in GaSb, corresponding to disorder-activated modes (DALA). The very weak intensity of these modes confirms the long-range order in the GaSb sublattice as discussed above.

Two bands can be distinguished above the frequency of the GaSb-like 2LO(Γ). The first band, between 490 and 560 cm^{-1}, contains combinations of GaSb-like and AlSb-like optical modes, and the second one, between 600 and 660 cm^{-1}, contains overtones of transverse AlSb-like optical modes at the zone centre, as well as possible contributions of overtones of longitudinal AlSb-like optical modes at the zone centre.

4. Conclusions

High-resolution first-order Raman spectra of the $Al_{0.14}Ga_{0.86}Sb$ alloy were recorded at room temperature and at 80 K. The spectra displayed two-mode behaviour and TO–LO splitting even for the AlSb-like modes despite the low Al content of the alloy. The values of TO–LO splitting of GaSb-like and AlSb-like modes suggest the occurrence of charge transfer from the less ionic Ga–Sb bond to the more ionic Al–Sb bond. The large width of the AlSb-like LO peak in relation to its GaSb-like counterpart reflects the short-range order of the AlSb sublattice. Conversely, the quite narrow GaSb-like peak indicates a high degree of structural order in the GaSb sublattice, according with previous reports of long-range order in other III–V alloys. The second-order Raman spectrum was also recorded. As expected from the alloy composition, the second-order spectrum is dominated by overtones and combinations of GaSb-like modes, although AlSb-like overtones and mixed GaSb-like and AlSb-like combinations were also identified.

Acknowledgment

We acknowledge the Spanish Ministerio de Educación y Ciencia for financial support.

References

[1] Munekata H, Mendez E E, Iye Y and Esaki L 1986 *Surf. Sci.* **174** 449
[2] Munekata H, Esaki L and Chang L L 1987 *J. Vac. Sci. Technol.* B **5** 809
[3] Munekata H, Smith T P III and Chang L L 1989 *J. Vac. Sci. Technol.* B **7** 325
[4] Beresford R, Luo L F and Wang W I 1989 *Appl. Phys. Lett.* **54** 1899
[5] Söderström J R, Chow D H and McGill T C 1989 *Appl. Phys. Lett.* **55** 1348
[6] Schulman J N, Chow D H and Hasenberg T C 1994 *Solid-State Electron.* **37** 981
[7] Inoue M, Yoh K and Nishida A 1994 *Semicond. Sci. Technol.* **9** 966
[8] Tsang W T and Olsson N A 1983 *Appl. Phys. Lett.* **43** 8
[9] Ohmori Y, Tarucha S, Horikoshi Y and Okamoto H 1984 *Japan. J. Appl. Phys.* **23** L94
[10] Lukovsky G, Cheng K Y and Pearson G L 1975 *Phys. Rev.* B **12** 4135
[11] Charfi F, Zouaghi M, Joullie A, Balkanski M and Hirlimann C 1980 *J. Physique* **41** 83
[12] Ahuja G, Gupta H C and Tiwari L M 1984 *Physica* B **124** 225
[13] Talwar D N, Vandevyver M and Zigone M 1981 *Phys. Rev.* B **23** 1743
[14] Bischopink G and Benz K W 1993 *J. Cryst. Growth* **128** 470
[15] Jusserand B and Sapriel J 1981 *Phys. Rev.* B **24** 7194
[16] Aoki K, Anastassakis E and Cardona M 1984 *Phys. Rev.* B **30** 681
[17] Hayes W 1964 *Phys. Rev. Lett.* **13** 275
[18] Lukovsky G, Brodsky M H and Burnstein E 1970 *Phys. Rev.* B **2** 3295

[19] Turner W J and Reese W E 1962 *Phys. Rev.* B **127** 126
[20] Talwar D N and Agrawal B K 1974 *Phys. Rev.* B **9** 2539
[21] Kuan T S, Kuech T F, Wang W I and Wilkie E L 1985 *Phys. Rev. Lett.* **54** 201
[22] Jen H R, Cherng M J and Stringfellow G B 1986 *Appl. Phys. Lett.* **48** 1603
[23] Shahid M A, Mahajan S and Laughlin D E 1987 *Phys. Rev. Lett.* **58** 2567
[24] Srivastava G P, Martins J L and Zunger A 1984 *Phys. Rev.* B **31** 2561
[25] Mikkelsen J C Jr and Boyce J B 1983 *Phys. Rev.* B **28** 7130
[26] *Landolt–Börnstein New Series* 1987 vol 22, ed O Madelung (Berlin: Springer)
[27] Farr M K, Traylor J G and Sinha S K 1975 *Phys. Rev.* B **11** 1587
[28] Banerjee R and Varshni Y P 1969 *Can. J. Phys.* **47** 451
[29] Klein P B and Chang R K 1976 *Phys. Rev.* B **14** 2498